MOLECULAR IMAGING AND BIOLOGY

Mol Imaging Biol (2019) 21:926–934
DOI: 10.1007/s11307-018-1300-1
© World Molecular Imaging Society, 2018
Published Online: 7 December 2018

RESEARCH ARTICLE

Quantification of Positron Emission Tomography Data Using Simultaneous Estimation of the Input Function: Validation with Venous Blood and Replication of Clinical Studies

Elizabeth A. Bartlett,[1] Mala Ananth,[2] Samantha Rossano,[3] Mengru Zhang,[4] Jie Yang,[5] Shu-fei Lin,[6] Nabeel Nabulsi,[6] Yiyun Huang,[6] Francesca Zanderigo,[7,8] Ramin V. Parsey,[1,9] Christine DeLorenzo[1,9]

[1]*Department of Biomedical Engineering, Stony Brook University, Stony Brook, NY, 11794, USA*
[2]*Department of Neuroscience, Stony Brook University, Stony Brook, NY, USA*
[3]*Department of Biomedical Engineering, Yale University, New Haven, CT, USA*
[4]*Department of Applied Mathematics and Statistics, Stony Brook University, Stony Brook, NY, USA*
[5]*Department of Family, Population, and Preventive Medicine, Stony Brook University, Stony Brook, NY, USA*
[6]*Department of Radiology & Biomedical Imaging, Yale University, New Haven, CT, USA*
[7]*Department of Psychiatry, Columbia University, New York, NY, USA*
[8]*Molecular Imaging and Neuropathology Division, New York State Psychiatric Institute, New York, NY, USA*
[9]*Department of Psychiatry, Stony Brook University, Stony Brook, NY, USA*

Abstract

Purpose: To determine if one venous blood sample can substitute full arterial sampling in quantitative modeling for multiple positron emission tomography (PET) radiotracers using simultaneous estimation of the input function (SIME).

Procedures: Participants underwent PET imaging with [^{11}C]ABP688, [^{11}C]CUMI-101, and [^{11}C]DASB. Full arterial sampling and additional venous blood draws were performed for quantification with the arterial input function (AIF) and SIME using one arterial or venous (vSIME) sample.

Results: Venous and arterial metabolite-corrected plasma activities were within 6 % of each other at varying time points. vSIME- and AIF-derived outcome measures were in good agreement, with optimal sampling times of 12 min ([^{11}C]ABP688), 90 min ([^{11}C]CUMI-101), and 100 min ([^{11}C]DASB). Simulation-based power analyses revealed that SIME required fewer subjects than the AIF method to achieve statistical power, with significant reductions for [^{11}C]CUMI-101 and [^{11}C]DASB with vSIME. Replication of previous findings and test-retest analyses bolstered the simulation analyses.

Conclusions: We demonstrate the feasibility of AIF recovery using SIME with one venous sample for [^{11}C]ABP688, [^{11}C]CUMI-101, and [^{11}C]DASB. This method simplifies PET

Electronic supplementary material The online version of this article (https://doi.org/10.1007/s11307-018-1300-1) contains supplementary material, which is available to authorized users.

Correspondence to: Elizabeth Bartlett; *e-mail:* Elizabeth.Bartlett@stonybrook.edu

acquisition while allowing for fully quantitative modeling, although some variability and bias are present with respect to AIF-based quantification, which may depend on the accuracy of the single venous blood measurement.

Key words: Venous blood, Less invasive PET, Simultaneous estimation, Sample size considerations

Introduction

Fully quantitative positron emission tomography (PET) relies on arterial blood sampling during the scan to measure the arterial input function (AIF), the unmetabolized radiotracer activity in blood needed to derive quantitative outcome measures (*e.g.*, total volume of distribution (V_T) and binding potentials) [1]. Arterial sampling is invasive, costly, and often a deterrent to subject enrollment and retention [2]. Methods that obviate such sampling, generally split into reference region and AIF recovery approaches, are invaluable. Reference region approaches solely quantify specific binding relative to nondisplaceable uptake (BP_{ND}), whereas alternate outcome measures can be needed, *e.g.*, V_T and specific binding relative to radiotracer in plasma (BP_P) [1]. Further, the assumption that there exists a reference region completely devoid of specific binding is not valid for many radiotracers, such as [^{11}C]DASB (target: serotonin transporter) [3], [^{11}C]ABP688 (target: metabotropic glutamate receptor 5) [4], [^{11}C]PE2I (target: dopamine transporter) [5], and [^{18}F]fallypride (target: dopamine D2/D3 receptor) [6]. Thus, less-invasive AIF recovery methods are of interest.

AIF recovery methods include population-based approaches, image-derived input functions [7–10], and simultaneous estimation (SIME) [2], which recovers the AIF using simultaneous fitting of PET data in multiple brain regions and one arterial blood sample, with the assumption that the AIF is common to all brain regions [11–14]. SIME has been applied to several radiotracers, including [^{11}C]DASB [2, 15], [^{11}C]PIB (for amyloid-beta fibrils) [2], [^{11}C]CUMI-101 [2, 16, 17] and [^{11}C]WAY-100635 [2, 17] (both for serotonin-1A receptor), and [^{18}F]FDG (glucose analog) [2, 12, 18].

Although methods such as SIME with one arterial sample (aSIME) require less blood to be drawn, they still necessitate arterial catheterization or puncture. Thus, venous blood-based quantification strategies are advantageous. If equivalence between venous and arterial metabolite-corrected radiotracer activity is demonstrated, venous blood could substitute arterial for less-invasive quantification. This has been shown for [^{18}F]FDG and [^{11}C]N-methylspiperone at late time points [19, 20]. As this equivalence likely varies by radiotracer, each radiotracer must be investigated independently.

Here, we determined the equivalence between venous and arterial plasma activity, parent fraction, and metabolite-corrected plasma activity for [^{11}C]ABP688, [^{11}C]CUMI-101, and [^{11}C]DASB and examined the use of a venous sample instead of an arterial in SIME (vSIME). This is the first SIME implementation for [^{11}C]ABP688. We hypothesized that venous-to-arterial metabolite-corrected plasma equivalence will be found at late time points and these points will provide optimal vSIME performance relative to AIF-based methods. An often overlooked consideration with less-invasive quantification methods is the impact on statistical power in clinical studies. Thus, we investigated the impact of SIME-based quantification on sample sizes required to detect group differences. We further sought to replicate previous AIF-based findings of diurnal variation with [^{11}C]ABP688 and test-retest repeatability with [^{11}C]CUMI-101 and [^{11}C]DASB.

Materials and Methods

Subjects

Table 1 displays information on participants and data. The Institutional Review Boards at Columbia, Stony Brook, and Yale Universities approved this study. Written, informed consent was received from each participant. Inclusion criteria were as follows: ages 18–70 years and capacity to provide informed consent (details reported in electronic supplementary material (ESM)), yielding 10, 19, and 18 scans for [^{11}C]ABP688, [^{11}C]CUMI-101, and [^{11}C]DASB, respectively, in which both arterial and venous sampling was performed. PET scans used to estimate optimal sampling time-points were independent of those in prior SIME validations.

PET Acquisition and Processing

Radiotracer preparation, image acquisition, pre-processing, and metabolite-corrected AIF (product of plasma and parent fraction) fitting were performed as previously described [3, 21–24] (for more details, see ESM).

SIME was employed as described elsewhere [2]. In brief, SIME minimizes an objective function that incorporates both AIF parameters and compartmental model parameters for several regions of interest (ROIs), and includes one blood sample as an anchor for model identifiability [2] (the ROIs used within SIME are reported in ESM).

SIME was ran with the arterial and venous metabolite-corrected activities in closest correspondence and with the

Table 1. Subject demographics, data acquisition, and analysis protocols

Radiotracer	# of subjects	Age	Number (%) female	Injected dose (mCi)	Arterial plasma draw time (min)	Venous plasma draw time (min)	Scan duration (min)	Modeling method; metabolite fit	Scanner
[^{11}C]ABP688	10	35.10 ± 9.86	5 (50 %) female	16.60 ± 2.68	4, 9, 12, 15, 20, 25, 30, 40, 50, 60	4, 12, 30, 60	60	2-tissue compartment modeling; Hills	ECAT HRRT
[^{11}C]CUMI-101	19	36.53 ± 14.48	8 (42.1 %) female	13.65 ± 4.86	3, 12, 20, 30, 45, 60, 75, 90, 105, 120	3, 12, 30, 60, 90	120	LEGA; Hills	ECAT HR+
[^{11}C]DASB	18	35.72 ± 15.07	4 (40 %) female	12.98 ± 4.29	3, 12, 30, 35, 50, 65, 80, 90, 100	3, 12, 20, 50, 80, 100	100	LEGA; damped biexponential	ECAT HR+

LEGA likelihood estimation in graphical analysis

optimal anchor points previously identified for [^{11}C]CUMI-101 and [^{11}C]DASB [2, 25]. All time-points available were tested as potential anchors for this first SIME validation with [^{11}C]ABP688.

PET Quantification

Likelihood estimation in graphical analysis (LEGA) ([^{11}C]DASB and [^{11}C]CUMI-101) [26] or two-tissue compartmental (2TC) modeling ([^{11}C]ABP688) [27] quantified V_T. Corresponding BP_{ND} estimates were computed indirectly with V_T of the pseudoreference region previously suggested for these tracers (cerebellar gray matter) [3, 28, 29]. The regions used to assess SIME performance are provided in ESM.

SIME Validation

The difference between the AIF- and SIME-derived estimates, normalized by the AIF-derived estimate, assessed the agreement between methods [2, 25]. The optimal venous and arterial sampling time-point for anchoring SIME was determined using V_T percentage difference mean and standard deviations, and bootstrapped linear regressions were fit between AIF- and SIME-generated estimates [30] (details on bootstrapping are reported in ESM). Analyses were performed in MATLAB 2017a (The MathWorks, Inc.; Natick, MA).

Power Analysis

To examine the detection of group differences with SIME, one ROI per radiotracer was selected to mimic hypothesis-testing scenarios ([^{11}C]ABP688: hippocampus, [^{11}C]CUMI-101: anterior cingulate cortex, [^{11}C]DASB: amygdala). Twenty percent and 5 % group differences were generated from the AIF-estimated data, and the relationships between AIF and SIME estimates, determined during validation, were used to simulate SIME-based group differences (see ESM for details on simulated power analyses).

Results

Venous-to-Arterial Comparison

The ratio of venous-to-arterial plasma activity approached equivalence at late time-points for all radiotracers (Fig. 1): 1.01 ± 0.05 at 60 min ([^{11}C]ABP688), 0.96 ± 0.07 at 90 min ([^{11}C]CUMI-101), 0.96 ± 0.10 at 100 min ([^{11}C]DASB). The [^{11}C]ABP688 parent fraction remained higher in venous than in arterial plasma (ratio range 1.34–1.41 from 4 to 60 min; Fig. 1), while parent fraction was approximately equivalent in venous and arterial plasma for [^{11}C]CUMI-101 and [^{11}C]DASB (ratio range 0.91–1.02; Fig. 1). The venous-to-arterial metabolite-corrected plasma activities approached equivalence at 12 min for [^{11}C]ABP688 (ratio = 1.03 ± 0.28) and increased thereafter, while the same ratio converged at the latest time-points for [^{11}C]CUMI-101 (ratio = 0.97 ± 0.11 at 90 min) and [^{11}C]DASB (ratio = 0.97 ± 0.21).

SIME V_T

vSIME estimated V_T with a bias below 15 %, on average, for all radiotracers, and the optimal blood time-points matched those with the closest metabolite-corrected venous-to-arterial equivalence (Table 2, Fig. 2).

The optimal vSIME sampling times varied from the optimal aSIME times for [^{11}C]CUMI-101 and [^{11}C]DASB, where earlier arterial draws at 30 and 80 min, respectively, yielded the most accurate aSIME outcomes (Table 2, Fig. 2). Generally, aSIME and vSIME overestimated V_T relative to the AIF method (slopes = 0.79 to 1.08, Fig. 3).

Power Analysis

Across radiotracers and a- and vSIME, when accounting for the bias to generate simulations as described in ESM, SIME required

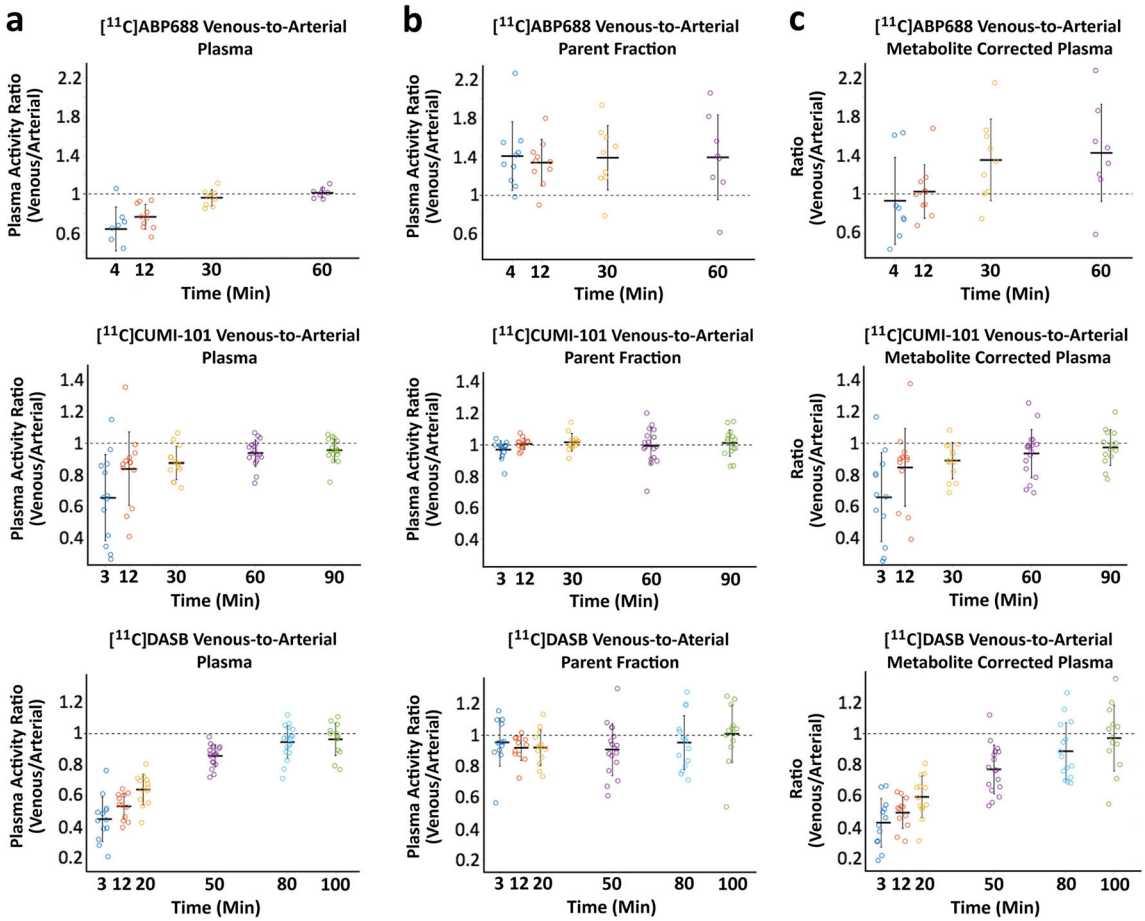

Fig. 1. **a** Venous-to-arterial ratios of total plasma activity. **b** Venous-to-arterial ratios of parent radiotracer fraction. **c** Venous-to-arterial ratios of metabolite-corrected plasma activity shown for all time- points across the three radiotracers. Mean and standard deviations are shown with horizontal and vertical solid lines. A ratio of 1 is shown with dashed lines in all plots.

fewer subjects to detect 20 % and 5 % group differences relative to the AIF method (Table 3). This reduction in sample size was significant for [^{11}C]CUMI-101 ($p = 0.004$ and 0.005 for 20 and 5 %, respectively) and [^{11}C]DASB ($p = 0.024$ and 0.045 for 20 and 5 %, respectively) with vSIME. For aSIME, only [^{11}C]DASB ($p = 0.010$ and 0.012 for 20 and 5 %, respectively) required significantly fewer subjects.

SIME BP_{ND}

At the optimal V_T-determined sampling times, aSIME and vSIME estimated BP_{ND} within 13 % and 10 %, respectively, of full sampling ([^{11}C]ABP688 −9.67 ± 20.7 % (aSIME) and −9.08 ± 19.46 % (vSIME); [^{11}C]CUMI-101 12.11 ± 7.59 % (aSIME) and 4.91 ± 21.08 % (vSIME); [^{11}C]DASB

Table 2. Percentage difference between simultaneous estimation (SIME)– and arterial input function–generated V_T across blood sampling times

Radiotracer	Sampling time (min)	Arterial				Venous			
		Mean ± SD	Median	MAD	[min, max]	Mean ± SD	Median	MAD	[min, max]
[^{11}C]ABP688	4	46.03 ± 9.13	49.62	4.49	[21.33, 59.41]	−131.99 ± 1212.69	31.02	24.11	[−1078.17, 71.40]
	12	*−5.88 ± 14.41*	*−8.77*	*8.36*	*[−28.85, 22.79]*	*−2.79 ± 18.69*	*−6.26*	*7.48*	*[−33.42, 42.44]*
	30	−72.80 ± 20.75	−66.65	12.12	[−116.91, −41.92]	−39.27 ± 43.80	−36.86	15.52	[−150.44, 28.85]
	60	−123.56 ± 51.28	−122.92	40.77	[−214.31, −35.29]	−69.41 ± 56.52	−47.42	13.04	[−241.26, 1.99]
[^{11}C]CUMI-101	*30*	*2.84 ± 11.74*	*3.79*	*7.05*	*[−25.41, 23.90]*	−15.35 ± 31.68	−15.33	12.06	[−248.72, 25.31]
	60	−1.30 ± 21.70	−5.16	7.47	[−37.01, 80.26]	−20.37 ± 19.93	−18.92	13.42	[−77.65, 16.86]
	90	−9.86 ± 24.20	−13.54	6.38	[−86.13, 78.01]	*−14.79 ± 24.09*	*−19.46*	*8.13*	*[−50.43, 67.85]*
[^{11}C]DASB									
	50	−8.51 ± 15.15	−10.84	4.33	[−40.01, 54.41]	−42.48 ± 29.04	−38.16	19.20	[−119.34, 24.32]
	80	*−8.00 ± 13.55*	*−7.03*	*9.61*	*[−39.22, 24.45]*	−20.90 ± 24.07	−23.67	14.49	[−76.58, 47.46]
	100	−12.40 ± 16.52	−6.71	12.79	[−59.38, 17.55]	*−11.66 ± 21.72*	*−9.72*	*6.96*	*[−86.18, 20.35]*

SD standard deviation, *MAD* median absolute deviation, V_T volume of distribution, Italics show the determined optimal time-points

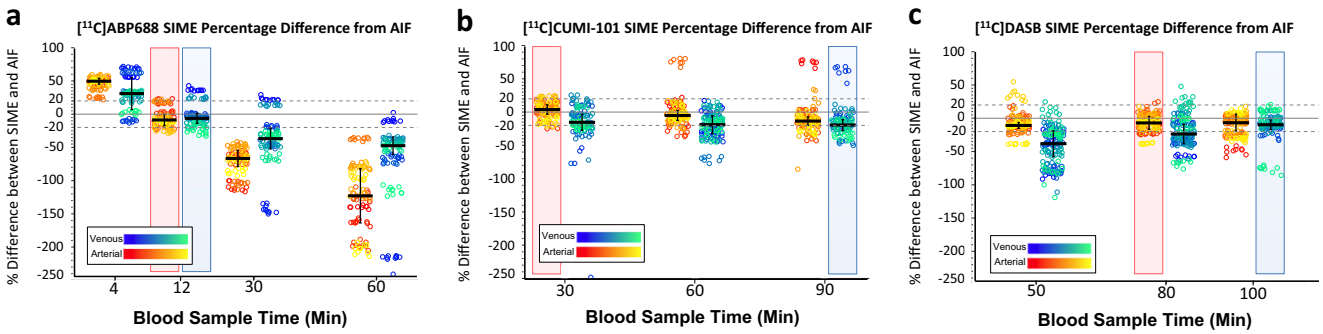

Fig. 2. Percentage differences between simultaneous estimation (SIME)– and arterial input function–derived V_T values shown for **a** [^{11}C]ABP688, **b** [^{11}C]CUMI-101, and **c** [^{11}C]DASB. The blood sampling times are shown on the *x*-axis. Arterial data is plotted left of the sampling time in red-to-yellow and venous is right in blue-to-green. Color gradients represent stratification by subject across the regions examined. Medians are shown with horizontal solid line and median absolute deviations (MADs) are shown with vertical solid lines. Two outliers are excluded from the 4-min venous sample plot for [^{11}C]ABP688, where percentage differences were – 5561.5 % and – 10,781.7 %. These points are included in the calculation of the medians and MADs.

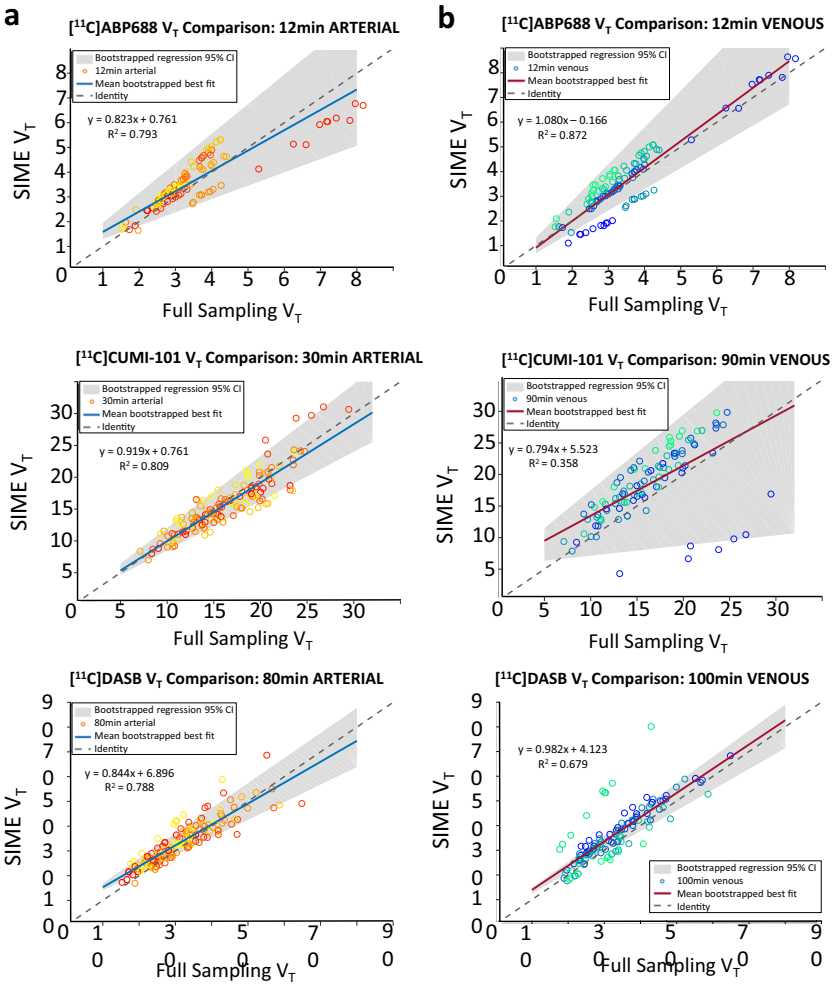

Fig. 3. V_T estimates from simultaneous estimation (SIME) and the arterial input function plotted for **a** the optimal arterial and **b** venous sampling times across the three radiotracers. Colors in the gradients from red-to-yellow and blue-to-green show individual subjects. Identity is shown with a black line. Mean best-fit approximation from bootstrapped regression is shown with a thick solid line. The 95 % bootstrapped regression confidence interval (CI) for the best-fit slope is shown in gray.

Table 3. Simulated group difference results

				Group difference = 20 %			Group difference = 5 %		
	Blood sample	Estimated slope of SIME *vs* AIF for the single region (mean ± SD)	Ratio of V_T variance (AIF/SIME)	Estimated sample size: SIME (mean ± SD)	Estimated sample size: AIF	*p* value	Estimated sample size: SIME (mean ± SD)	Estimated sample size: AIF	*p* value
[^{11}C]ABP688	Arterial	1.031 ± 0.367	1.795	35 ± 23	51	0.255	458 ± 324	807	0.17
	Venous	0.692 ± 0.225	0.740	37 ± 25	51	0.310	485 ± 339	807	0.2
[^{11}C]CUMI-101	Arterial	0.705 ± 0.103	0.624	12 ± 4	16	0.108	169 ± 62	244	0.119
	Venous	0.244 ± 0.303	0.397	6 ± 4	18	0.004*	93 ± 76	274	0.005*
[^{11}C]DASB	Arterial	0.750 ± 0.299	2.030	6 ± 3	14	0.010*	82 ± 49	210	0.012*
	Venous	0.354 ± 0.225	0.721	5 ± 2	9	0.024*	60 ± 37	130	0.045*

SIME simultaneous estimation, *AIF* arterial input function method, *SD* standard deviation
*$p < 0.05$

9.05 ± 9.98 % (aSIME) and 9.37 ± 9.62 % (vSIME)). Analogous to V_T estimation, BP_{ND} was overestimated (slopes = 0.79 to 0.93), although the 95 % confidence intervals (CIs) of the regression slopes were narrower and intercepts were lower than those of V_T, indicating higher accuracy in estimating BP_{ND} (Suppl. Fig. A in ESM) with this indirect approach.

Replicating Findings with [^{11}C]ABP688

DeLorenzo *et al.* [22] found significantly higher [^{11}C]ABP688 V_T in the afternoon relative to the morning when using AIF-based quantification. We sought to replicate these findings with SIME. Using 7 of the 8 published subjects (1 subject did not have venous sampling and was excluded here) [22], a significant effect of time-of-day was found with AIF-based quantification for V_T ($p = 0.001$, $\beta = 0.78$), but not for BP_{ND} ($p = 0.17$), with afternoon uptake higher than morning uptake, agreeing with published results [22].

Using aSIME and vSIME, these findings were replicated for V_T (aSIME: $p = 0.001$, $\beta = 1.60$; vSIME: $p < 0.001$; $\beta = 1.17$) and BP_{ND} (aSIME: $p = 0.24$; vSIME: $p = 0.08$).

Replicating Test-Retest Findings

Scans from independent test-retest studies were used ([^{11}C]CUMI-101 8 subjects and [^{11}C]DASB 12 subjects with test and same-day retest scans), which overlap with the 7 [^{11}C]CUMI-101 scans and the 11 [^{11}C]DASB scans reported in previous studies [21, 31]. Only aSIME was assessed because venous samples were not collected in the previous studies.

For [^{11}C]DASB, absolute test-retest percent differences using an AIF were 8.92 ± 8.53 % (V_T) and 13.79 ± 17.00 % (BP_{ND}). With aSIME, test-retest variability increased to 18.93 ± 14.69 % (V_T) and 13.53 ± 17.94 % (BP_{ND}). A significant difference was found in test-retest variability in V_T between SIME and AIF, but not in BP_{ND} (V_T: $p = 0.03$, 10.01 % higher variability with aSIME; BP_{ND}: $p = 0.90$, 0.26 % lower variability with aSIME).

For [^{11}C]CUMI-101, absolute test-retest percent differences using an AIF were 6.90 ± 4.56 % (V_T) and 14.14 ± 9.63 % (BP_{ND}). With aSIME, variability increased to 9.66 ± 7.89 % (V_T) and 15.56 ± 11.65 % (BP_{ND}). There were no significant differences in test-retest variabilities between AIF and aSIME (V_T: $p = 0.26$, 2.76 % higher variability with aSIME; BP_{ND}: $p = 0.53$, 1.43 % higher variability with aSIME).

Discussion

The purpose of this investigation across the radiotracers [^{11}C]ABP688, [^{11}C]CUMI-101, [^{11}C]DASB was to (1) report the radiotracer dynamics in venous plasma relative to arterial, (2) validate the use of one venous blood sample for full quantification with SIME, and (3) illustrate the applicability of SIME in future studies. Our results indicate that venous and arterial metabolite-corrected plasma activities approached equivalence for all three radiotracers, albeit at different times post-injection. One venous sample generated outcome measures with good agreement to AIF-based quantification. Next, we found that SIME requires comparable, or even smaller, sample sizes, relative to AIF-based quantification, to accurately detect group differences. These effects were bolstered with analyses seeking to replicate prior findings.

Venous-to-Arterial Plasma Comparison

This blood data was examined in the context of choosing optimal post-injection blood sampling times for SIME, although it can be used to further: (1) other less-invasive quantification techniques and (2) our understanding of the mechanisms underlying radiotracer metabolism.

Across radiotracers, we observed higher total activity in arterial relative to venous plasma early in the scan and equilibration by the end of the scan. We found that [^{11}C]ABP688 parent fraction was higher in venous plasma

than in arterial plasma throughout the scan; because this ratio was stably higher than 1, it was at 12 min post-injection, when the venous-to-arterial total plasma activity was lower than 1, that the corresponding venous and arterial metabolite-corrected plasma activities approximated each other. The relative deficit of radiometabolites observed in venous plasma appears to be biological. Examination of the high-pressure liquid chromatography (HPLC) data for venous and arterial plasma revealed clear separation of parent and metabolite peaks, despite a potential for pH-related differences in HPLC retention [32]. It is however difficult to identify potential biological explanations for this parent fraction imbalance. One possibility is that constant metabolite sequestration by the liver for excretion (80 % of [^{11}C]ABP688 excretion is hepatobiliary [27]) may contribute to there being less metabolites in venous than in arterial plasma. The fact that the arterial-to-venous equivalence of metabolite-corrected plasma activity is reached *via* the canceling of an overestimation and underestimation is not ideal. One potential solution requiring validation is to normalize the venous parent fraction by the constant bias observed throughout the scan.

For [^{11}C]CUMI-101 and [^{11}C]DASB, given a relatively stable ratio of venous-to-arterial parent fraction (~ 1) throughout the scan, the metabolite-corrected plasma activities equilibrated at late time-points, when the raw plasma activity, initially higher in arterial plasma, approached venous.

SIME Validation

We provide the first validation of SIME for [^{11}C]ABP688, while we build upon previous work validating aSIME for [^{11}C]CUMI-101 and [^{11}C]DASB. We found that the optimal venous sampling times were those with the closest metabolite-corrected plasma activity correspondence between venous and arterial blood (12, 90, and 100 min for [^{11}C]ABP688, [^{11}C]CUMI-101, and [^{11}C]DASB, respectively). SIME with blood samples acquired at these optimal times estimated V_T within 15 % of the AIF method.

For [^{11}C]ABP688, vSIME was slightly more accurate in estimating V_T than aSIME (percentage difference from the AIF method − 2.8 % for vSIME and − 5.9 % for aSIME), with the optimal blood sample time at 12 min.

For [^{11}C]CUMI-101 and [^{11}C]DASB, aSIME was previously found to optimally estimate V_T with a blood sample acquired at 60 and 50 min, respectively [2, 16, 25], while here, we found that the optimal time points were 30 and 80 min, respectively. This discrepancy may be attributable to different considered datasets and selection criteria (signed percent difference normalized by AIF-derived values used here, while unsigned percent difference normalized by the average of the two measurements used previously [2]). The fact that all late-scan time points provided accurate quantification (within 13 %), however, provides flexibility in applying aSIME to previously acquired datasets.

Although it is important to additionally examine binding potential estimation to test if SIME is robust to quantifying specific binding, when binding potentials are computed *via* subtraction or normalization, like here, with a reference region, biases introduced with SIME may be removed or reduced. As expected, BP_{ND} (as compared to V_T) was more stably estimated with SIME relative to full sampling, as evidenced by narrower ranges of regression slopes, higher R-squared values, and narrower CIs. Cerebellar gray matter has been shown to exhibit some specific binding for these tracers and is thus not an ideal reference region [3, 28, 33, 34], so BP_{ND} estimates with full sampling and SIME will both be biased [35]. To remediate this bias, approaches have been proposed to estimate BP_{ND} noninvasively without a reference region [17, 36], but further binding potential estimation validation with SIME is necessary.

Power Analysis

Less-invasive PET quantification methods have the potential to reduce accuracy and precision in estimating outcomes [37]. Importantly, introduced bias and variance can negatively impact statistical power to detect group differences, an issue which is often unaddressed.

We found that when SIME group differences are simulated based on the established bias between SIME and AIF-based estimates, SIME required smaller sample sizes than the AIF method to achieve statistical power, with significant reductions observed for vSIME with [^{11}C]CUMI-101 and [^{11}C]DASB and for aSIME with [^{11}C]DASB. This effect can be understood by examining the bias and variance introduced with SIME. For example, for [^{11}C]CUMI-101 in Table 3, the slope relating vSIME to AIF-based estimates was 0.24, indicating a large V_T overestimation with vSIME. The variance in V_T was also greater with vSIME than with full sampling (ratio of variance = 0.40; Table 3). However, the variance in V_T does not appear to scale linearly with its overestimation, yielding a group difference that is visually, and statistically, more discernable (see Suppl. Fig. B.a and Table A in ESM).

Conversely, vSIME with [^{11}C]ABP688 (Suppl. Fig. B.b and Table A in ESM) slight overestimations were observed in V_T and V_T variance; thus, statistical power did not significantly differ between vSIME and full sampling. Importantly, the relationship between SIME and full sampling must be known and considered when weighing SIME's utility within varying study designs. If alternate blood sampling times are used or this relationship was to change otherwise, then sample sizes would need to be reassessed.

Replication of Findings

As fewer subjects were required in the simulation analyses to achieve statistical power, we hypothesized that SIME

would be powered to estimate larger group differences in diurnal variation of [^{11}C]ABP688 V_T than full sampling. vSIME and aSIME estimated significant diurnal variations in [^{11}C]ABP688 V_T, replicating previous AIF-based findings [22], but the magnitude of the diurnal variation was overestimated with SIME. While DeLorenzo *et al.* observed weak, but significant, effects with BP_{ND}, SIME and AIF using 7 of the 8 original subjects yielded nonsignificant diurnal variations with BP_{ND}. This may be a result of reduced statistical power using fewer subjects in this study, as the direction of the diurnal variation—afternoon uptake higher than morning—was consistent across all current and prior analyses [22]. These data support the simulation-based analyses, but while group differences are detectable with SIME, absolute estimates of V_T, as well as the magnitude of group-wise effects, are not necessarily estimated precisely.

SIME did not significantly alter test-retest variability in V_T or BP_{ND} relative to AIF-based quantification for [^{11}C]CUMI-101, supporting the nonsignificant difference in sample sizes detected in the simulation-based analyses. With [^{11}C]DASB, however, aSIME significantly increased the test-retest variability of V_T by 10 % over the AIF method, but provided BP_{ND} test-retest repeatability within 0.3 % of the AIF method. Notably, for [^{11}C]DASB, vSIME V_T values are in closer agreement to AIF values than aSIME (vSIME slope = 0.98; aSIME slope = 0.84). Future analyses on [^{11}C]DASB test-retest datasets with venous blood may reveal that vSIME can robustly generate V_T estimates with lower test-retest variability.

Limitations

When weighing the reduced cost and burden relative to AIF-based quantification, without the need to increase sample sizes, SIME is a promising less-invasive approach. However, given the limited sample sizes considered, future validation is needed. Future work might also consider using more physiological models for the AIF, such as pharmacokinetic models [15]. Further, given that the optimal venous blood sampling times are 90 and 100 min for [^{11}C]CUMI-101 and [^{11}C]DASB, respectively, and that these tracers are carbon-11 labeled, it is possible that metabolite measurements may be less reliable at these late time-points, perhaps contributing to the relatively low correlation observed between vSIME and AIF-based V_T for these radiotracers. A potential solution to be investigated is to obtain and average duplicate or triplicate plasma and parent fraction measurements at the defined sampling time-point, which may enhance the suboptimal V_T correspondence, and be especially advantageous if lower activity doses are injected.

[^{11}C]CUMI-101 and [^{11}C]DASB samples were composed of healthy control and depressed patients, and SIME performance was not found to significantly differ across the populations (see details in ESM). Despite these preliminary results, we recommend validation of venous-to-arterial blood equivalence for specific populations/treatments before use in a large study, as this equivalence could vary across conditions.

Conclusions

Less-invasive PET quantification methods, like SIME, are essential to mitigate costs and discomfort associated with AIF-based quantification. We found that at the optimal blood sampling time, venous blood can substitute the previously validated arterial sample in SIME to provide outcomes in agreement with AIF-based quantification for [^{11}C]ABP688, [^{11}C]CUMI-101, and [^{11}C]DASB. One limitation is the observed variability in SIME performance across subjects, which may be related to the accuracy of venous blood measurement used for SIME anchoring. Future work could investigate acquisition of repeated blood draws at the anchor time to stabilize potential uncertainty introduced with a single plasma activity and parent fraction measurement. Further, work to develop noninvasive derivations of the SIME anchor could obviate the need for any blood sampling [15, 16].

Pivotal to assessing the utility of a less-invasive method, SIME-introduced bias did not decrease statistical power. However, the fact that a bias is observed in the current SIME implementation necessitates careful consideration before application to studies in need of absolute quantification of outcomes. Despite this bias, however, SIME replicated previous findings of diurnal variation in [^{11}C]ABP688 binding and test-retest reliability of [^{11}C]CUMI-101 and [^{11}C]DASB binding and, thus, may be a promising alternative for minimally invasive PET quantification.

Acknowledgments. We thank the Center for Understanding Biology using Imaging Technology image analysts at Stony Brook University for their work in image importing, processing, and quality control. We also thank Rajapillai Pillai, PhD, for his contributions to early versions of the paper. We acknowledge the consultation and support provided by the Biostatistical Consulting Core at the Stony Brook University School of Medicine.

Funding. This study was funded by the National Institute of Mental Health awards: K01MH091354 (PI: Christine DeLorenzo, PhD), R01MH104512 (PI: Christine DeLorenzo, PhD), and R01MH090276 (PI: Ramin V Parsey, MD, PhD).

Compliance with Ethical Standards

Conflict of Interest

The authors declare that they have no conflict of interest.

Ethical Approval

All procedures performed were in accordance with the ethical standards of the institutional committee and with the 1964 Helsinki Declaration and its later amendments.

Informed Consent

Informed consent was obtained from all individual participants included in the study.

Publisher's Note Springer Nature remains neutral with regard to jurisdictional claims in published maps and institutional affiliations.

References

1. Innis RB, Cunningham VJ, Delforge J et al (2007) Consensus nomenclature for in vivo imaging of reversibly binding radioligands. J Cereb Blood Flow Metab 27:1533–1539
2. Ogden RT, Zanderigo F, Choy S et al (2010) Simultaneous estimation of input functions: an empirical study. J Cereb Blood Flow Metab 30:816–826
3. Parsey RV, Kent JM, Oquendo MA et al (2006) Acute occupancy of brain serotonin transporter by sertraline as measured by [11C]DASB and positron emission tomography. Biol Psychiatry 59:821–828
4. Ametamey SM, Treyer V, Streffer J et al (2007) Human PET studies of metabotropic glutamate receptor subtype 5 with 11C-ABP688. J Nucl Med 48:247–252
5. DeLorenzo C, Kumar JS, Zanderigo F et al (2009) Modeling considerations for in vivo quantification of the dopamine transporter using [(11)C]PE2I and positron emission tomography. J Cereb Blood Flow Metab 29:1332–1345
6. Ishibashi K, Robertson CL, Mandelkern MA, et al. (2013) The simplified reference tissue model with 18F-fallypride positron emission tomography: choice of reference region. Mol Imaging 12
7. Takikawa S, Dhawan V, Spetsieris P et al (1993) Noninvasive quantitative fluorodeoxyglucose PET studies with an estimated input function derived from a population-based arterial blood curve. Radiology 188:131–136
8. Fung EK, Carson RE (2013) Cerebral blood flow with [15O]water PET studies using an image-derived input function and MR-defined carotid centerlines. Phys Med Biol 58:1903–1923
9. Su Y, Arbelaez AM, Benzinger TL et al (2013) Noninvasive estimation of the arterial input function in positron emission tomography imaging of cerebral blood flow. J Cereb Blood Flow Metab 33:115–121
10. Zanotti-Fregonara P, Chen K, Liow JS et al (2011) Image-derived input function for brain PET studies: many challenges and few opportunities. J Cereb Blood Flow Metab 31:1986–1998
11. Sanabria-Bohórquez SM, Labar D, Levêque P et al (2000) [11 C] Flumazenil metabolite measurement in plasma is not necessary for accurate brain benzodiazepine receptor quantification. Eur J Nucl Med 27:1674–1683
12. Guo H, Renaut RA, Chen K (2007) An input function estimation method for FDG-PET human brain studies. Nucl Med Biol 34:483–492
13. Riabkov DY, Di Bella EV (2002) Estimation of kinetic parameters without input functions: analysis of three methods for multichannel blind identification. IEEE Trans Biomed Eng 49:1318–1327
14. Wong KPMS, Dagan F, Fulham MJ (2002) Estimation of input function and kinetic parameters using simulated annealing application in a flow model. IEEE Trans Nucl Sci 49:707–713
15. Mikhno A, Zanderigo F, Todd Ogden R et al (2015) Toward noninvasive quantification of brain radioligand binding by combining electronic health records and dynamic PET imaging data. IEEE J Biomed Health 19:1271–1282
16. Zanderigo F, Ogden RT, Parsey RV (2015) Noninvasive blood-free full quantification of positron emission tomography radioligand binding. J Cereb Blood Flow Metab 35:148–156
17. Schain M, Zanderigo F, Mann JJ, Ogden RT (2017) Estimation of the binding potential BPND without a reference region or blood samples for brain PET studies. NeuroImage 146:121–131
18. Roccia E, Mikhno A, Zanderigo F, et al. (2015) Non-invasive quantification of brain [(18)F]-FDG uptake by combining medical health records and dynamic PET imaging data. Conference proceedings : Annual International Conference of the IEEE Engineering in Medicine and Biology Society IEEE Engineering in Medicine and Biology Society Annual Conference 2015:2243–2246
19. Wakita K, Imahori Y, Ido T et al (2000) Simplification for measuring input function of FDG PET: investigation of 1-point blood sampling method. J Nucl Med 41:1484–1490
20. Wong DF, Wagner HN Jr, Tune LE et al (1986) Positron emission tomography reveals elevated D2 dopamine receptors in drug-naive schizophrenics. Science 234:1558–1563
21. Milak MS, DeLorenzo C, Zanderigo F et al (2010) In vivo quantification of human serotonin 1A receptor using 11C-CUMI-101, an agonist PET radiotracer. J Nucl Med 51:1892–1900
22. DeLorenzo C, Kumar JS, Mann JJ, Parsey RV (2011) In vivo variation in metabotropic glutamate receptor subtype 5 binding using positron emission tomography and [^{11}C]ABP688. J Cereb Blood Flow Metab 31:2169–2180
23. Wu S, Ogden RT, Mann JJ, Parsey RV (2007) Optimal metabolite curve fitting for kinetic modeling of 11C-WAY-100635. J Nucl Med 48:926–931
24. Parsey RV, Ojha A, Ogden RT et al (2006) Metabolite considerations in the in vivo quantification of serotonin transporters using 11C-DASB and PET in humans. J Nucl Med 47:1796–1802
25. Zanderigo F, Ogden RT, Mann JJ, Parsey RV (2010) A voxel-based clustering approach for the automatic selection of testing regions in the simultaneous estimation of input functions in PET [abstract]. 52: S176P
26. Ogden RT (2003) Estimation of kinetic parameters in graphical analysis of PET imaging data. Stat Med 22:3557–3568
27. Treyer V, Streffer J, Wyss MT et al (2007) Evaluation of the metabotropic glutamate receptor subtype 5 using PET and 11C-ABP688: assessment of methods. J Nucl Med 48:1207–1215
28. DeLorenzo C, Milak MS, Brennan KG et al (2011) In vivo positron emission tomography imaging with [(1)(1)C]ABP688: binding variability and specificity for the metabotropic glutamate receptor subtype 5 in baboons. Eur J Nucl Med Mol Imaging 38:1083–1094
29. Milak MS, Severance AJ, Ogden RT et al (2008) Modeling considerations for 11C-CUMI-101, an agonist radiotracer for imaging serotonin 1A receptor in vivo with PET. J Nucl Med 49:587–596
30. Efron B, Tibshirani R (1986) Bootstrap methods for standard errors, confidence intervals, and other measures of statistical accuracy. Stat Sci:54–75
31. Ogden RT, Ojha A, Erlandsson K et al (2007) In vivo quantification of serotonin transporters using [(11)C]DASB and positron emission tomography in humans: modeling considerations. J Cereb Blood Flow Metab 27:205–217
32. Malatesha G, Singh NK, Bharija A et al (2007) Comparison of arterial and venous pH, bicarbonate, PCO2 and PO2 in initial emergency department assessment. Emerg Med J 24:569–571
33. Parsey RV, Arango V, Olvet DM et al (2005) Regional heterogeneity of 5-HT1A receptors in human cerebellum as assessed by positron emission tomography. J Cereb Blood Flow Metab 25:785–793
34. Turkheimer FE, Selvaraj S, Hinz R et al (2012) Quantification of ligand PET studies using a reference region with a displaceable fraction: application to occupancy studies with [(11)C]-DASB as an example. J Cereb Blood Flow Metab 32:70–80
35. Salinas CA, Searle GE, Gunn RN (2015) The simplified reference tissue model: model assumption violations and their impact on binding potential. J Cereb Blood Flow Metab 35:304–311
36. Todd Ogden R, Zanderigo F, Parsey RV (2015) Estimation of in vivo nonspecific binding in positron emission tomography studies without requiring a reference region. NeuroImage 108:234–242
37. Slifstein M, Laruelle M (2001) Models and methods for derivation of in vivo neuroreceptor parameters with PET and SPECT reversible radiotracers. Nucl Med Biol 28:595–608